Unmanned Systems, Vol. 14, No. 4 (2026) 913–926

DOI: 10.1142/S2301385026500263

UNMANNED SYSTEMS
https://www.worldscientific.com/worldscinet/us

Nonlinear Model Predictive Control of Tilt-Rotor UAV Under a Dual Differential Model Based on INDI Strategy

Tianrui Fang, Changping Du*, Rui Yang, Yuean Wu, Jiahao Yu, Zean Du, Yiming Shang, Yao Zheng

School of Aeronautics and Astronautics, Zhejiang University, Hangzhou 310027, Zhejiang, P. R. China

This paper proposes a new tilt-rotor UAV (TRUAV) that integrates the hovering capabilities of quadrotors with the long-range flight benefits of fixed-wing aircraft. Designed with a dual differential rotor architecture, this TRUAV enhances energy efficiency and obstacle avoidance capabilities. Given the challenges posed by the TRUAV's highly coupled and nonlinear dynamic characteristics in attitude and tilt angle control, a controller integrating Incremental Nonlinear Dynamic Inversion (INDI) control with Nonlinear Model Predictive Control (NMPC) has been designed. This controller achieves precise trajectory tracking and attitude control through NMPC while utilizing the INDI strategy for real-time computation of rotor tilt angles during the transition mode. To optimize energy usage and enhance maneuverability and obstacle avoidance capabilities, a novel introduction of Front-Back and Left-Right rotor differential modes has been implemented. Experimental results show that the NMPC controller based on the INDI strategy can effectively handle the complex dynamics of TRUAV and achieve efficient control performance in attitude control. Compared to the traditional PID, the proposed controller reduces the maximum pitch angle of the TRUAV during flight by 34.60%, achieving an 11.44% improvement over the conventional NMPC method.

Keywords: Tilt-rotor UAV (TRUAV); nonlinear model predictive control (NMPC); incremental nonlinear dynamic inversion (INDI); trajectory tracking; attitude control.

US

1. Introduction

Unmanned Aerial Vehicles (UAVs) integrate wireless communication, image processing, and various sensing technologies into unmanned aircraft. These aircraft can be remotely controlled and can also perform autonomous flights. UAV can undertake tasks that are dangerous for human operators or too costly for manned aviation [1]. In recent years, the extensive application of UAV in civil, military, and industrial fields, such as surveillance, search and rescue, high-altitude intelligence reconnaissance, environmental monitoring, weather research, pipeline inspection, and natural disaster risk management, has garnered significant attention [2,3]. Today, over 1,000 UAV models are being developed in over 50 countries, serving as indispensable assistants for human operators in a broad range of military and civil applications [4].

In the field of aviation, fixed-wing aircraft and rotorcraft each play important roles due to their unique advantages. Fixed-wing aircraft are characterized by longer flight ranges, lower noise, and higher cruising speeds but require runways for takeoff and cannot hover vertically. In contrast, rotorcraft can hover at fixed positions but have lower cruising speeds and endurance. Tilt-rotor UAV, which combine high-speed cruising and vertical takeoff and landing (VTOL) capabilities, have attracted significant interest from researchers due to their rapid, long-range, and vertical takeoff capabilities. TRUAV can achieve two to three times the flight speed and range of conventional rotorcraft, along with excellent transport capabilities [5].

Tilt-rotor UAV feature rotor modes, fixed-wing modes, and transition modes, allowing them to perform vertical takeoffs and landings, hover in place, and cruise at high speeds, as shown in Fig. 1. During flight, the rotor mode primarily relies on propellers for power, while the transition

Received 24 September 2024; Revised 10 March 2025; Accepted 11 March 2025; Published 5 May 2025. This paper was recommended for publication in its revised form by editorial board member, Jinqiang Cui.
Email Addresses: *duchangping@zju.edu.cn
*Corresponding author.

Fig. 1. The three flight modes of TRUAV.

Fig. 2. Changes in tilt angle throughout the flight process.

mode is facilitated by a tiltable rotor system, typically mounted on the wings, and can adjust its tilt angle based on flight speed. As flight speed increases and the lift provided by the wings gradually increases, the rotors fully transition to a horizontal position, shifting the UAV into fixed-wing mode for flight, as shown in Fig. 2.

With the advancement of UAV control technology and the continuous development of new aircraft design concepts, various configurations of tilt-rotor aircraft have been proposed. For example, the XV-15 and V-22 tilt-rotor aircraft designed by Bell Helicopter in the United States feature two tiltable rotors mounted at the wingtips [6]. The Swiss Federal Institute of Technology Zurich (ETH Zurich) proposed a Tri-TRUAV, which consists of a pair of front tiltable rotors and a single rear tiltable rotor [7]. The École Polytechnique Fédérale de Gambinie proposed a Quad-TRUAV, which has two pairs of tiltable rotors mounted at the front and rear of the fuselage [8]. The Japan Aerospace Exploration Agency developed a UAV with rotors mounted in the middle of the wings, and both the wings and rotors can tilt together [9]. Researchers of Delft University of Technology proposed a novel combination of a quadrotor and a hybrid biplane capable of joint hover and joint forward flight [10].

Despite the significant advantages and broad application prospects of TRUAV, they still face many technical challenges, especially in dynamics modeling and attitude control during transition modes. As the rotors tilt, the UAV exhibits complex aerodynamic characteristics, such as strong aeroelastic coupling and pronounced nonlinearity, which significantly increase the difficulty of modeling and controller design. In terms of dynamic modeling, the transition mode requires switching between rotor mode and fixed-wing mode and adjusting the pitch, roll, and yaw attitude of the TRUAV [11]. During low-speed flight, the aerodynamic forces of the fixed wings are less influential, and the rotor's flight characteristics are mainly considered. However, at high speeds, the aerodynamics of the wings play a dominant role. This requires simultaneous consideration of the dynamic characteristics of both rotors and fixed wings in the modeling, and coordination of control surfaces and thrust vectoring, thereby increasing the complexity of operation and control systems. Consequently, attitude controller design for TRUAV in transition flight states is more challenging than in other states [12].

To achieve the transition process in TRUAV, scholars have employed various methods to design flight controllers. Sato designed a PID controller to control the altitude and attitude of quad-tilt-wing unmanned aerial vehicles [13]. However, the PID method performed poorly with strongly nonlinear control subjects, requiring the simultaneous design of multiple controllers to complete the transition process. Small *et al.* designed a control structure based on cascaded P-PI and PID to adjust the hovering performance of the Tilt-Wing UAV and conducted simulation experiments under various noise and interference scenarios [14]. Muraoka and L. Bauersfeld designed two sets of controllers for the rotor mode and fixed-wing mode of TRUAV, distributing control weights through gain scheduling [15]. Hamiss *et al*. designed a nonlinear feedback controller to control the speed and attitude of an aircraft [16]. Facing the strongly nonlinear model of TRUAV, Zhao *et al*. linearized the mathematical model at multiple equilibrium points and proposed a hierarchical controller. The upper layer uses state variables to determine the choice of lower layer controllers, while the lower layer designs robust controllers to control the models at each equilibrium point, achieving mode transition [17]. Xian *et al*. proposed a sliding mode controller suitable for small UAV, which can compensate for unmodeled flapping dynamics and external disturbances but cannot completely avoid input chattering [18]. Ma *et al*. developed an adaptive flight control system to compensate for modeling uncertainties caused by loads [19]. Müller *et al*. developed a novel tilt-wing UAV and employed the Incremental Nonlinear Dynamic Inversion (INDI) control strategy to regulate its attitude.

Tilt-rotor aircraft exhibit significant nonlinearity due to their complex dynamics and the necessity to switch between various flight modes. To maintain aircraft attitude stability during mode transitions, NMPC, as an extended form of MPC, can handle a wider range of system dynamics and achieve more powerful control performance in nonlinear systems. In practical applications, the tilt angle of the rotors is usually adjusted in real-time according to the current flight objectives and the UAV's attitude. NDI and INDI methods simplify the design of controllers under system uncertainties and external disturbances, significantly improving controller performance [20, 21]. Through the INDI method, the required tilt angle can be calculated in real-time during TRUAV flight and used as a reference for NMPC tracking to optimize control objectives.

Most of the current literature focuses on the control issues of TRUAV during forward tilting and aircraft acceleration, while little research is dedicated to reverse tilting and

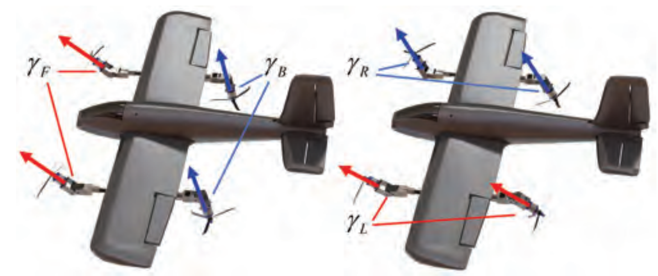

Fig. 3. (a) Front-Back model. (b) Left-Right model.

deceleration. Additionally, once the rotors have tilted, the aircraft is solely treated as a fixed-wing aircraft, overlooking the tilt angle as a potentially valuable control variable. A TRUAV model with Front-Back and Left-Right rotor differential settings is proposed in this paper, providing better attitude control during the tilt transition mode and enabling maneuverable obstacle avoidance in fixed-wing mode, as shown in Fig. 3.

In summary, this paper focuses on the design of an NMPC controller based on the INDI strategy for attitude control and trajectory tracking during the tilt-transition and fixed-wing modes of TRUAV under a highly nonlinear dual-differential model. The controller is designed to manage the entire operational cycle of TRUAV, and its efficacy is confirmed through comparative flight experiments against traditional PID and MPC methods.

The remainder of the paper is organized as follows. Section 2 establishes the six-degree-of-freedom nonlinear motion model for the TRUAV. Section 3 designs the NMPC controller based on the INDI tilting strategy, with a focus on the selected state input variables and controller constraints. Sections 4 and 5 involve flight testing and comparative analysis of results.

The main contributions of this paper are summarized as follows:

(i) A dual differential rotor model for TRUAVs: A novel model is proposed, featuring distinct control strategies for different flight modes. The front-back rotor tilt differential operates in rotor and transition modes, which stabilizes attitude during the tilt transition. It enables smooth and reliable mode switching. The left-right rotor tilt differential for fixed-wing mode improves aerodynamic efficiency and reduces turning radius, especially enhancing maneuverability during obstacle avoidance.

(ii) An integrated INDI-NMPC control strategy: A novel control architecture combines the INDI method with NMPC. INDI computes adaptive tilt angles in real time, providing robust disturbance rejection and adaptability to dynamic flight conditions. NMPC utilizes these angles for precise trajectory tracking and attitude control, ensuring high accuracy and stability especially in complex scenarios. The synergy between INDI and NMPC results in a highly efficient and robust control framework.

2. TRUAV Mathematical Model

The coordinate frames involved in the tilt-rotor unmanned aerial vehicle and TRUAV's basic structure studied in this

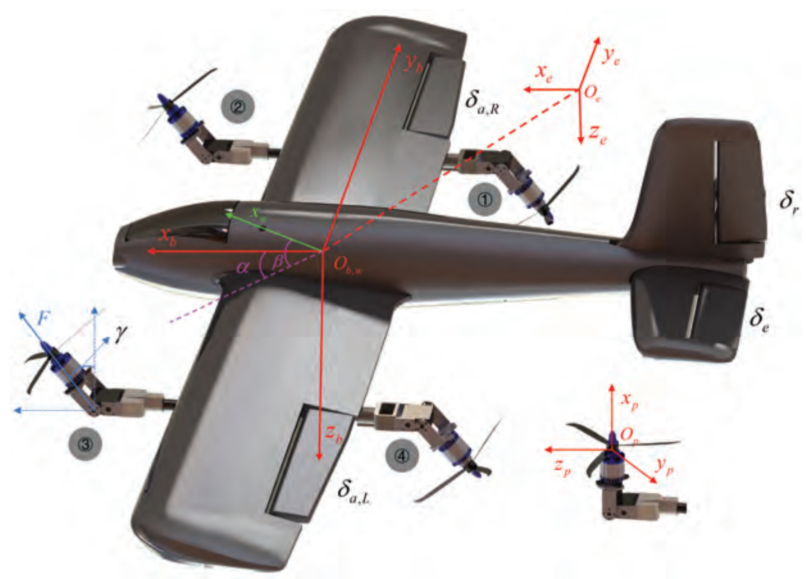

Fig. 4. Coordinate frames and basic structure.

paper are shown in Fig. 4. [22]:

(i) Flight Path Coordinate Frame $O_e x_e y_e z_e$
(ii) Body Coordinate Frame $O_b x_b y_b z_b$
(iii) Propeller Shaft Coordinate Frame $O_p x_p y_p z_p$
(iv) Airflow Coordinate Frame $O_w x_w y_w z_w$

To accurately describe the dynamic characteristics of the tilt-rotor UAV while avoiding excessive complexity, the following assumptions are introduced before modeling individual components:

(i) The mass and mass distribution of the tilt-rotor UAV are uniform and do not change over time.
(ii) The tilt-rotor UAV is treated as a rigid body, and the elastic deformation of the airframe is ignored.

This TRUAV is equipped with four propellers that provide thrust, along with conventional control surfaces such as elevators, rudders, and ailerons. Additionally, each propeller is equipped with a servo to accomplish tilting. By precisely controlling these actuators, the TRUAV can smoothly transition between different flight modes and achieve effective control. According to the earlier assumptions, the aircraft is a rigid body in three-dimensional space, the mathematical model under the body coordinate frame can be described according to Newton–Euler's laws [23].

$$\begin{aligned} \dot{P} &= R_{be}^T V_b, \\ \dot{V}_b &= -\Omega_b \times V_b + \frac{T_b}{m}, \\ \dot{\Theta} &= W(\phi, \theta, \varphi)\Omega_b, \\ \dot{\Omega}_b &= J^{-1}[M_b - \Omega_b \times (J \cdot \Omega_b)], \end{aligned} \tag{1}$$

where $\times$ denotes the cross product of two vectors; $P = [x\ y\ x]^T$ is the position vector in the flight path coordinate frame, $V_b = [V_x\ V_y\ V_z]^T$ is the velocity vector in the body coordinate frame, $\Omega_b = [p\ q\ r]^T$ is the angular velocity vector in the body coordinate frame, m and J are the mass and inertia matrix, respectively, $T_b \in \mathbb{R}^{3\times1}$ and $M_b \in \mathbb{R}^{3\times1}$ are the resultant force vector and torque vector in the body coordinate frame. Forces and torques are provided by the rotors, wings, and tail.

$$\begin{aligned} T_b &= T_r + T_a + R_{be}G, \\ M_b &= M_r + M_a, \end{aligned} \tag{2}$$

where $T_r \in \mathbb{R}^{3\times1}$ and $M_r \in \mathbb{R}^{3\times1}$ are the thrust and torque generated by the rotors on the airframe, respectively; $T_a \in \mathbb{R}^{3\times1}$ and $M_a \in \mathbb{R}^{3\times1}$ are the aerodynamic force and aerodynamic torque acting on the fuselage; $G \in \mathbb{R}^{3\times1}$ is gravity; $R_{be} \in \mathbb{R}^{3\times3}$ is the direction cosine matrix from the flight path coordinate frame to the body coordinate frame, which is related to the roll, pitch, and yaw attitudes. The transpose R_{be}^T is the transformation matrix from the body coordinate frame to the flight path coordinate frame.

$$R_{be} = \begin{bmatrix} C_\theta C_\psi & C_\theta S_\psi & -S_\theta \\ S_\phi S_\theta C_\psi - S_\psi C_\phi & S_\phi S_\theta S_\psi + C_\phi C_\psi & S_\phi C_\theta \\ C_\phi S_\theta C_\psi + S_\psi S_\phi & C_\phi S_\theta S_\psi - S_\phi C_\psi & C_\phi C_\theta \end{bmatrix}. \tag{3}$$

(i) Rotor Force and Torque Model

The propellers of the TRUAV are driven by direct current motors. Therefore, the propeller model:

$$\begin{aligned} t_i &= C_T \rho A r^2 \omega^2, \\ M_i &= C_Q \rho A r^2 \omega |\omega|, \end{aligned} \tag{4}$$

where t_i and τ are the thrust and torque produced by a propeller, C_T and C_Q are dimensionless constants representing the thrust coefficient and torque coefficient, respectively. ρ is the air density, A is the rotor disk area of the propeller, and ω is the rotational speed of the propeller.

The total thrust T_r generated by the rotors is the sum of the thrust vectors produced by the four propellers, with different modeling methods under various differential model architectures.

In the rotor mode and tilt-transition mode, there is differential variation between the front and rear rotors:

$$T_r = (t_1 + t_4)\begin{bmatrix} \sin(\gamma_F) \\ 0 \\ -\cos(\gamma_F) \end{bmatrix} + (t_2 + t_3)\begin{bmatrix} \sin(\gamma_B) \\ 0 \\ -\cos(\gamma_B) \end{bmatrix}. \tag{5}$$

In fixed-wing mode, the differential variation between the front and rear rotors is

$$T_r = (t_1 + t_2)\begin{bmatrix} \sin(\gamma_R) \\ 0 \\ -\cos(\gamma_R) \end{bmatrix} + (t_3 + t_4)\begin{bmatrix} \sin(\gamma_L) \\ 0 \\ -\cos(\gamma_L) \end{bmatrix}, \tag{6}$$

where γ is the tilt angle, with subscripts F and B denoting the front and back pairs of propellers, respectively. Subscripts L and R are the left and right pairs of propellers. The total torque M_r generated by the rotors is produced by both the propeller thrust and the reaction torque, as shown in Fig. 5.

$$M_r = \sum_{i=1}^{4} [R_{br} M_i + d_{ri} \times t_i], \tag{7}$$

where R_{br} is the transformation matrix from the rotor coordinate frame to the body coordinate frame, and d_{ri} is the position vector from the TRUAV's center of gravity to the point of action of the propeller thrust. d_{ri} can be expressed

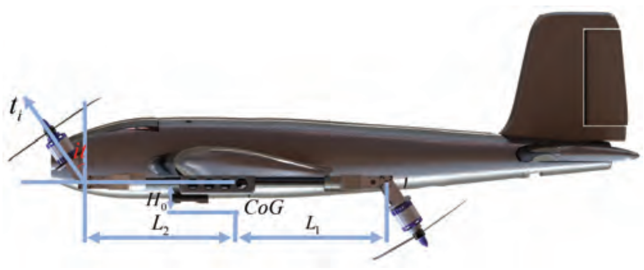

Fig. 5. Propeller installation structure.

as

$$\begin{aligned} d_{r1} &= [-L_2\ L_0\ -H_0]^T, \\ d_{r2} &= [L_1\ L_0\ -H_0]^T, \\ d_{r3} &= [L_1\ -L_0\ -H_0]^T, \\ d_{r4} &= [-L_2\ -L_0\ -H_0]^T. \end{aligned} \tag{8}$$

(ii) Wing Force and Torque Model

During flight, the aerodynamic force generated by the airflow passing over the aircraft's wing surfaces is

$$\begin{aligned} L &= qSC_L(\alpha), \\ Y &= qSC_Y(\beta), \\ D &= qSC_D(\alpha), \end{aligned} \tag{9}$$

$$T_A = [-D\ \ Y - L]^T, \tag{10}$$

Table 1. Physical parameters of TRUAV.

Name	Parameter	Value	Unit
Aircraft mass	m	8	kg
Inertia	J_{xx}	0.7316	kg·m^2
	J_{yy}	1.0664	kg·m^2
	J_{zz}	1.6917	kg·m^2
Air density	ρ	1.225	kg/m^3
Gravity coefficient	g	9.81	N/m
Wingspan	d	2	m
Surface area of main wing	$S_{\text{main wing}}$	0.6617	m^2
Surface area of elevator	S_{elevator}	0.0656	m^2
Surface area of aileron	S_{aileron}	0.0844	m^2
Surface area of rudder	S_{rudder}	0.0428	m^2
Elevator chord length	b	0.1	m
Aileron chord length	a	0.1	m
Rudder chord length	c	0.08	m
Maximum tilt angle	$\gamma_{\max}$	90	°
Minimum tilt angle	$\gamma_{\min}$	−7	°
Tilt plane y-offset	L_0	0.52	m
Front thrust point	L_2	0.105	m
Back thrust point	L_1	0.115	m
Tilt mechanism z-offset	H_0	0.015	m
Propeller thrust coefficient	C_T	1.99017×10^{-7}	
Propeller torque coefficient	C_Q	1.11917×10^{-5}	

where L is the lift, Y is the side force, D is the drag, $q = \frac{1}{2}\rho V^2$ is the dynamic pressure, V is the airspeed, S is the wing area, α is the angle of attack, β is the sideslip angle, $C_L(\alpha)$ and $C_D(\alpha)$ are the lift and drag coefficients related to the angle of attack, respectively. $C_Y(\beta)$ is the side force coefficient associated with the sideslip angle.

(iii) Actuator

The aerodynamic torque M_a generated by the control surfaces is collectively produced by the ailerons, elevators, and rudder.

$$M_a = qS[C_{L,a}\delta_a a\ C_{M,e}\delta_e b\ C_{N,r}\delta_r c]^T. \tag{11}$$

The physical parameters of TRUAV are shown in Table 1.

3. Flight Controller

During the transition phase, TRUAV needs to maintain the stability of its flight altitude and attitude and quickly complete structural changes to shorten the transition time. These requirements make controller design difficult. To tackle these challenges, a tilt strategy based on INDI is proposed in this paper. This strategy adaptively adjusts the propeller tilt angle according to the flight objectives and current flight state and employs the NMPC method to precisely control the aircraft's position and attitude.

3.1. *Tilt strategy plan*

The adaptive tilt angle strategy of the TRUAV is crucial for maintaining flight altitude and attitude stability, especially during the smooth transition between flight modes. The INDI method achieves the transition between flight modes by real-time adjustment of the tilt angle. In the vertical takeoff and landing mode, the rotors are perpendicular to the ground to provide lift to assist the TRUAV in ascending and hovering, while in the transition to fixed-wing mode, the rotors gradually move to a horizontal position to optimize thrust and lift output. The adaptability of the INDI method allows the TRUAV to automatically adjust the tilt angle during flight mode transitions, thus maintaining stable flight altitude and attitude. The advantage of this method is that it effectively manages transition flight and mode switches without requiring a predefined trajectory of rotor tilt angle changes over time.

The virtual control variables generated by the rotors are denoted as $U = [U_1\ U_2\ U_3]^T$, used to control the TRUAV's forward, longitudinal and pitch movements. U_1 and U_2 are the components of the rotor thrust in the body coordinate frame, and U_3 is the torque generated by the thrust difference between the front and rear pairs of rotors. Through the distribution matrix in Eq. (12), the virtual control variables are resolved into the thrust components of the front and rear rotors.

$$\begin{bmatrix} T_{x,F}^{\text{des}} \\ T_{z,F}^{\text{des}} \\ T_{x,B}^{\text{des}} \\ T_{z,B}^{\text{des}} \end{bmatrix} = \begin{bmatrix} \frac{1}{2} & 0 & 0 \\ 0 & \frac{L_1}{L_1+L_2} & -\frac{1}{L_1+L_2} \\ \frac{1}{2} & 0 & 0 \\ 0 & \frac{L_2}{L_1+L_2} & \frac{1}{L_1+L_2} \end{bmatrix} U, \tag{12}$$

where the subscripts F and B are the front and rear rotors, respectively, while T_X and T_z denote the forward and longitudinal force components generated by the rotors. The adaptive tilt angles γ_F for the front propellers and γ_B for the rear propellers can be calculated:

$$\begin{aligned} \gamma_F &= \arctan\left(\frac{T_{x,F}^{\text{des}}}{T_{z,F}^{\text{des}}}\right), \\ \gamma_B &= \arctan\left(\frac{T_{x,B}^{\text{des}}}{T_{z,B}^{\text{des}}}\right). \end{aligned} \tag{13}$$

The INDI method is proposed in the paper to solve the virtual control variables. The INDI method incrementally processes the system's dynamic equations, mapping the system's output increments to the required input increments. Information related to the controlled object model is replaced by measurable system states, reducing model dependency. Unmodeled effects and disturbances can be directly measured and compensated for in the next control increment [24].

The overall structure of the adaptive TRUAV tilt strategy and flight controller based on velocity and attitude is shown in Fig. 6.

3.1.1. *INDI-based velocity controller*

The INDI-Based Velocity Controller consists of a linear velocity controller, an incremental dynamic inversion module, and a real-time inverse matrix solver. It receives the velocity commands during tilting and the real-time state of the TRUAV, solving for acceleration differences and the inverse matrix. The virtual control variables are solved in the incremental dynamic inversion module and attitude commands are

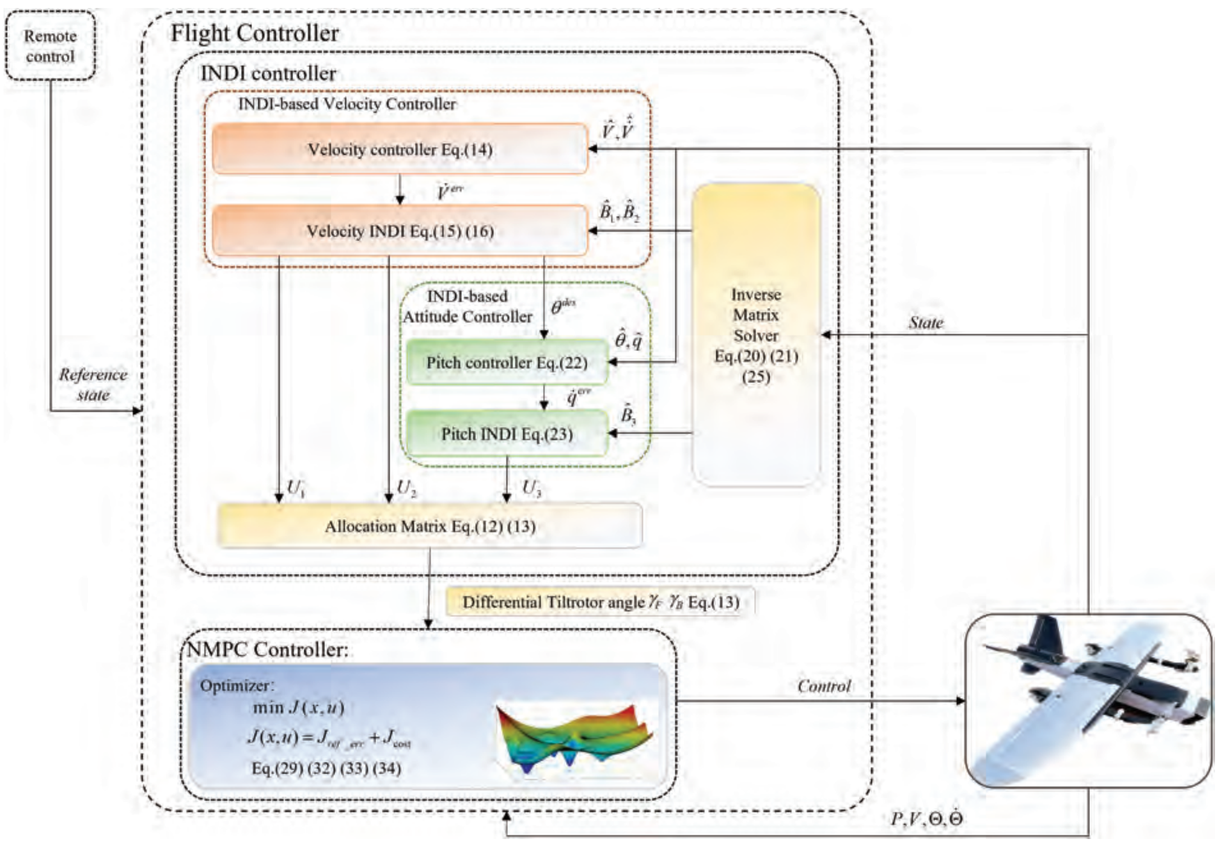

Fig. 6. Control diagram gives an overview over the whole control architecture of the vehicle. The flight controller includes two parts: the INDI controller and the NMPC controller. The INDI controller computes the adaptive tilt strategy. This tilt angle is then conveyed to the NMPC controller, which computes the optimal control strategy for the given tilt angle.

output to the INDI-Based Attitude Controller. The specific functions of each module are as follows:

(i) Linear Velocity Controller

The linear velocity controller takes the desired velocity, current velocity, and acceleration as inputs, using PID to convert the velocity difference into the required acceleration to eliminate the velocity tracking error of the TRUAV. The result is then differenced with the current body acceleration and passed on to the incremental dynamic inversion module.

(ii) Incremental Dynamic Inversion Module

In the incremental dynamic inversion solution, the nonlinear system state equations for the body velocity in the x_b and Z_b axes are first determined. The virtual control variables F_x and F_z are selected as the thrust components provided by the rotors. The pitch angle θ is chosen as the control variable to change the angle of attack of the airflow over the wings, thereby altering the TRUAV's longitudinal acceleration. Based on the principles of INDI control theory [22], the model for the TRUAV's acceleration in the x and z directions is formulated as follows:

$$\begin{bmatrix}\dot{V}_x\\ \dot{V}_z\end{bmatrix} = \bar{f}(x) + \hat{B}_1\begin{bmatrix}U_1\\ U_2\end{bmatrix} + \hat{B}_2\begin{bmatrix}0\\ \theta\end{bmatrix}, \tag{14}$$

where $\bar{f}(x)$ is the system state equation related to acceleration. B_1 and B_2 are controller coefficients derived from the real-time inverse matrix solver. Due to the strong coupling and nonlinear dynamic characteristics of the TRUAV in the tilt transition mode, $\bar{f}(x)$ has model errors, leading to poor control performance. However, based on INDI theory, which does not require an exact model, the virtual control variables can be written as

$$\begin{bmatrix}U_1\\ \tilde{U}_2\end{bmatrix} = \begin{bmatrix}U_1'\\ U_2'\end{bmatrix} + \hat{B}_1^{-1}(\dot{V}^{\text{des}} - \hat{\dot{V}}), \tag{15}$$

$$\tilde{\theta}^{\text{des}} = \theta' + \hat{B}_2^{-1}(\dot{V}_z^{\text{des}} - \hat{\dot{V}}_z), \tag{16}$$

$$\dot{V}^{\text{err}} = \dot{V}^{\text{des}} - \hat{\dot{V}}, \tag{17}$$

where U_1', U_2' and θ' are the control and state variables from the previous torque, with the superscripts on $\tilde{U}_2$ and $\tilde{\theta}^{\text{des}}$ indicating that they require mixed control processing. $\hat{B}_1$ and $\hat{B}_2$ are the coefficient matrices solved by the real-time inverse matrix solver based on the current state. $\dot{V}^{\text{des}}$ is the intermediate value solved by the linear velocity controller, and $\dot{V} = [\dot{V}_x\ \dot{V}_z]^T$ is the real-time acceleration value of the TRUAV.

$$\begin{bmatrix}\theta^{\text{des}}\\ U_2\end{bmatrix} = \begin{bmatrix}\tilde{\theta}^{\text{des}}k\\ \tilde{U}_2(1-k)\end{bmatrix}, \tag{18}$$

$$\begin{cases} k = 0 & V < 5,\\ k = \dfrac{1}{2}\left[1 - \cos\left(\dfrac{\pi}{16}(V-5)\right)\right] & 5 \le V < 21,\\ k = 1 & V \ge 21. \end{cases} \tag{19}$$

(iii) Real-Time Inverse Matrix Solver

The real-time inverse matrix solver receives instantaneous state data from the TRUAV and calculates control coefficients through mechanistic analysis and a single perturbation numerical method. As U_1 and $U2$, respectively, represent the forward and longitudinal forces, the control coefficients are determined to be $1/m$ based on Newton's laws of motion. Changes of θ alter the gravitational and aerodynamic forces on the wings, thus the control coefficients in the real-time inverse matrix solver are determined using the single perturbation numerical method as follows:

$$\hat{B}_1 = \frac{1}{m}I_{2\times 2}, \tag{20}$$

$$\hat{B}_2 = \frac{\partial V_z}{\partial \theta} = \frac{\partial V_z}{\partial G}\cdot\frac{\partial G}{\partial \theta} + \frac{\partial V_z}{\partial L}\cdot\frac{\partial L}{\partial \theta} + \frac{\partial V_z}{\partial D}\cdot\frac{\partial D}{\partial \theta}. \tag{21}$$

After inverting the coefficient matrices, they are substituted into Eqs. (15) and (16) in the incremental dynamic inversion module, resulting in the values of U_1, U_2 and θ^{des}. Then θ^{des} is passed to the controller INDI-Based Attitude Controller.

3.1.2. *INDI-based attitude controller*

The configuration of the INDI-Based Attitude Controller is essentially the same as that of the INDI-Based Velocity Controller, also consisting of a linear attitude controller, an incremental dynamic inversion module, and a real-time inverse matrix solver. It receives the pitch angle command from the INDI-Based Velocity Controller during tilting and the real-time state of the TRUAV, solving for the pitch angle acceleration difference and the inverse matrix. The virtual control variable U_3 is solved in the incremental dynamic inversion module. The specific functions of each module are as follows:

(i) Linear Attitude Controller

The linear attitude controller is the same as the linear velocity controller, using the PID to eliminate the tracking errors of the pitch angle and its angular velocity.

(ii) Incremental Dynamic Inversion Module

The pitch of the TRUAV is controlled jointly by the torque generated by the rotors and the elevators, with the virtual control variable U_3 chosen as the pitch torque provided by the rotors, thus the control model aimed at pitch angle acceleration can be written as

$$\dot{q} = \bar{f}(x) + \hat{B}_3U_3 + \hat{B}_4\delta_e, \tag{22}$$

where $\bar{f}(x)$ is the system state matrix related to pitch angle acceleration, while $\hat{B}_3$ and $\hat{B}_4$ are the coefficients for the rotors and elevators regarding pitch angular velocity. Since the incremental dynamic inversion method only requires control coefficients related to the control variables, the control command of propeller thrust can be written as

$$\tilde{U}_3 = U_3' + \hat{B}_3^{-1}(\dot{q}^{\text{des}} - \hat{\dot{q}}), \tag{23}$$

where U_3' is the control variable from the previous torque. $\tilde{U}_3$ requires mixed control with the elevator surface. $\hat{B}_3^{-1}$ is the inverse coefficient solved in real-time. $\dot{q}^{\text{des}}$ is the difference between $\dot{q}^{\text{des}}$ and $\hat{\dot{q}}$. It is evident that the advantage of INDI lies in its ability to operate without the need to model or solve for $\bar{f}(x)$ and $\hat{B}_4$, thus reducing the difficulties and errors associated with modeling. Similarly, by incorporating the mixed control rate Eq. (19), the rotor's control over the attitude gradually weakens as the level flight speed increases.

$$U_3 = \hat{U}_3(1 - k). \tag{24}$$

(iii) Real-Time Inverse Matrix Solver

Similar to the real-time inverse matrix solver in the velocity INDI module, the real-time inverse matrix solver receives real-time state quantities from the TRUAV and solves the control coefficient $\hat{B}_3$ through mechanism analysis. Since the virtual control variable U_3 is the pitch torque, the control coefficient for U_3 is written as

$$\hat{B}_3 = \frac{1}{J_{yy}}. \tag{25}$$

After inverting the coefficient matrix, it is substituted into Eq. (23) of the incremental dynamic inversion module to solve for the virtual control variable.

As the flight speed increases, the lift grows. When the lift can balance the gravity, the rotors no longer need to provide thrust in the z_b direction, and thus $U_2 = 0$. According to the mixed control algorithm of the tilt-rotor and elevators, when the flight speed is high, the rotors no longer participate in pitch attitude control $U_3 = 0$. It is clear from the distribution matrix that at this time $T_z = 0$, the rotors are completely tilted, and the thrust direction points forward. This means that as the flight speed continues to increase, the effect of the elevators is enhanced, allowing the rotors to gradually tilt to the horizontal position of the aircraft, while still meeting the current requirements of the tilt transition phase.

3.2. *NMPC controller*

The INDI method calculates real-time adaptive propeller tilt angles and passes them to the NMPC controller. This section will explore the application of NMPC throughout the entire flight process of the TRUAV, covering stages such as vertical takeoff, tilt acceleration, level flight maneuvering, reverse tilt deceleration, to vertical descent. The goal is to achieve precise trajectory tracking and ensure stability of attitude throughout the process.

For discrete-time nonlinear systems, the system's state function can be expressed as [25]

$$x(k+1) = f(x(k), u(k)), \quad x(0) = x_0, \tag{26}$$

where $f : \mathbb{R}^n \times \mathbb{R}^m \to \mathbb{R}^n$ is locally Lipschitz continuous, describing the dynamic behavior of the discrete system at discrete time $k \geq 0$, as shown in Fig. 7. $x(k) \in R^n$ and $u(k) \in R^m$ are the state and input vectors at time k. Subject to input and state constraints of the following form:

$$\begin{aligned} x(k) &\in \mathcal{X}, \quad \forall k \geq 0, \\ u(k) &\in \mathcal{U}, \quad \forall k \geq 0, \end{aligned} \tag{27}$$

where X and U are convex sets of the following form:

$$\begin{aligned} \mathcal{X} &= \{x \in \mathbb{R}^n \mid x_{\min} \leq x \leq x_{\max}\}, \\ \mathcal{U} &= \{u \in \mathbb{R}^m \mid u_{\min} \leq u \leq u_{\max}\}. \end{aligned} \tag{28}$$

It involves constant vectors $x_{\min}$, $x_{\max}$ and $u_{\min}$, $u_{\max}$.

$$\begin{aligned} &\underset{u}{\text{minimize}} \\ &\text{subject to:} \\ &\qquad x(k+1) = f(x(k), u(k)), \\ &\qquad x(k) \in \mathcal{X}, \quad \forall k \in [0, N], \\ &\qquad u(k) \in \mathcal{U}, \quad \forall k \in [0, N-1], \\ &\qquad x(0) = x_0. \end{aligned} \tag{29}$$

3.2.1. *Input and output vectors*

In controller design, selecting appropriate state vectors and input vectors is a crucial step. To optimize computational efficiency, only those physical quantities that are significant

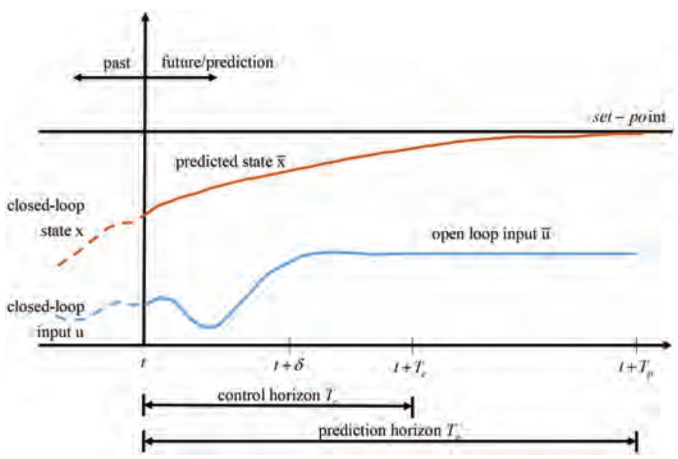

Fig. 7. Principle of model predictive control.

for the evaluation of flight performance are chosen. Considering the system's dynamic characteristics, operational objectives, constraints and the feasibility of practical applications, it has been decided to include position, forward velocity, attitude and rotor tilt angle as part of the state vector. The corresponding input vectors include rotor speed, control surface actions and the rotational speed of the tilt motors. This design strategy ensures that the control system can meet the requirements of the flight mission while also maintaining computational efficiency.

$$\begin{aligned} x &= [P \quad \Theta \quad V_x \quad \gamma]^T \in \mathbb{R}^9, \\ u &= [t_{1,2,3,4} \quad \delta_{a,e,r} \quad \bar{\gamma}]^T \in \mathbb{R}^8, \end{aligned} \tag{30}$$

where γ and $\bar{\gamma}$ change as the differential model changes.

In rotor mode and tilt transition mode: $\gamma = [\gamma_F \; \gamma_B]^T$.

In fixed-wing mode: $\gamma = [\gamma_L \; \gamma_R]^T$.

$\bar{\gamma}$ is the corresponding rotational speed of the tilt motor. The state vectors selected by this method contain variables that can affect the system's future behavior, and the chosen input vectors can effectively drive the system to achieve the desired performance indicators, ensuring the system's observability and controllability.

3.2.2. *Constraints*

The main advantage of Model Predictive Control (MPC) is that it allows for the imposition of constraints on inputs and states, which is crucial for ensuring the stability, safety, and efficiency of the system. The optimization problem in the predictive method is formulated so that the path and dynamics are considered equality and inequality constraints [26]. MPC ensures that the system operates within a safe and reliable range by setting reasonable constraints. During the flight control process of TRUAV, constraints are applied to the maximum and minimum tilt angles and tilt speeds of the rotors based on the physical limits of the tilt servos. By employing appropriate output and state constraints, MPC helps guide the system toward the desired performance level. The specific input and state constraints designed for TRUAV are as follows:

$$\begin{aligned} &|\Theta| < \begin{bmatrix} \frac{\pi}{4} & \frac{\pi}{4} & \infty \end{bmatrix}^T, \quad \gamma \in [-7,\ 90] \text{ deg}, \\ &|V| < [30 \quad 5 \quad 5]^T, \quad \bar{\gamma} \in [-15,\ 15] \text{ deg}^{-1}, \\ &t_i \in [0,\ 30] \text{ N}, \quad \delta_{a,e,r} \in [-30,\ 30] \text{ deg}. \end{aligned} \tag{31}$$

3.2.3. *Cost function*

In nonlinear model predictive control, the setting of the cost function is central to the control strategy. The cost function defines the objectives that the controller needs to achieve and optimize, and its selection has a direct impact on control performance. Through appropriate weighting, the cost function not only optimizes control performance but also enhances system robustness. To ensure accurate reference tracking, the designed cost function $J(x, u)$ includes a cost $J_{\text{ref\_err}}$ associated with tracking errors in position and velocity, as well as an input cost J_{cost} aimed at maintaining a stable attitude and achieving energy optimization. The chosen cost function adopts a quadratic form to effectively balance performance and cost.

$$J(x, u) = J_{\text{ref\_err}} + J_{\text{cost}}. \tag{32}$$

(i) Reference Tracking Error

To minimize the difference between the system's output and the predetermined targets, the position and velocity tracking errors are penalized in the form of squared sums, assisting the TRUAV in achieving the predefined operating conditions.

$$J_{\text{ref\_err}} = \sum_{k=0}^{N-1} (x - x_{\text{ref}})^T Q (x - x_{\text{ref}}). \tag{33}$$

In this model, N is the length of the prediction horizon that the cost function needs to minimize, and $Q = \text{diag}(Q_x \; Q_{V_x} \; Q_y \; Q_z \; Q_{\gamma_1} \; Q_{\gamma_2})$ is a weight vector used to gauge the importance of different performance indicators. In vertical takeoff and level flight maneuvering modes, the system focuses on tracking the referenced position input to ensure minimal positional deviation during vertical takeoffs and landings. In the tilt transition mode guided by INDI, the control strategy prioritizes tracking the TRUAV's forward speed and flight altitude to align with INDI's tilt plan. By adjusting the weights of the elements in Q, the response priority of the TRUAV can be regulated in the face of disturbances and uncertainties. Particularly during the tilt transition phase, to maintain efficient and stable altitude tracking, a higher Q_z weight will be set. Such configurations help ensure the stability and efficiency of the flight process.

(ii) State and Input Cost

The cost of state and inputs is calculated from the squared sum of each element of the aircraft's attitude and input vector, weighted by quadratic terms. Throughout the entire flight process of the TRUAV, the objective is to keep the aircraft's attitude vector close to zero values and to limit the magnitude of control actions to promote efficient energy savings. This cost setting helps optimize the aircraft's energy efficiency while maintaining precision and stability in operations.

$$J_{\text{cost}} = \sum_{k=0}^{N-1} (\Theta^T Q_\Theta \Theta + u^T R u). \tag{34}$$

Table 2. NMPC parameters.

State and control		Flight mode		
		Rotor	transition	Fixed-wing
	x	6	0	2
	y	3	5	10
Q	z	10	10	10
	V_x	0	5	0
	γ_1	3	5	1
	γ_2	3	5	1
	ϕ	6	6	1
Q_Θ	θ	10	10	2
	ψ	7	7	1
	u_1	0.4	0.4	0.4
	u_2	0.4	0.4	0.4
	u_3	0.4	0.4	0.4
	u_4	0.4	0.4	0.4
	δ_a	0.05	0.01	0.01
R	δ_e	0.05	0.01	0.01
	δ_r	0.05	0.01	0.01
	$\bar{\gamma}_1$	0.8	0.05	0.05
	$\bar{\gamma}_1$	0.8	0.05	0.05

The values of the diagonal matrices Q_Θ and R are listed in Table 2.

4. Flight Test Results

To comprehensively and thoroughly evaluate the performance of the proposed controller in different TRUAV modes and its advantages over other controllers, three experiments were designed: (1) TRUAV takes off in rotor mode and completes the transition mode switch. (2) Obstacle avoidance using the differential model of left and right propellers in fixed wing mode. (3) The full flight process, including takeoff–transition–fixed wing–transition–landing. The controller is based on the INDI tilt strategy and applies to TRUAVs with a dual-differential model. The TRUAV is shown in Fig. 8.

Fig. 8. Object picture.

4.1. *Tilt process experiment*

In the flight experiments, the TRUAV took off vertically from its initial position on the ground and stabilized at a hovering altitude of 10 m. At 10 s, the rotors began to tilt forward, completing a change from 0° to 90° within 10 s. Meanwhile, the flight speed reached 21 m/s. After the tilt was completed, the TRUAV entered fixed-wing mode.

This experiment visually demonstrates the significant differences between the INDI-NMPC control method and the PID control method. In the PID control strategy, the tilt angle γ is preset to change linearly over time. In contrast, the INDI-NMPC method uses an adaptive INDI tilt strategy, which adjusts the reference value of the tilt angle in real-time based on current speed and attitude, and introduces a differential model for the rotors' fore and aft movements, as shown in Fig. 11. Under PID control, the aircraft needs to pitch down significantly during acceleration to obtain the forward component of thrust, and substantial changes in roll and yaw angles cause fluctuations in altitude and lateral position during the tilt process, as shown in Fig. 10. According to Fig. 9, the comparative flight experiments demonstrate that the INDI-NMPC method exhibits significant advantages in controlling the TRUAV. As evidenced by the error bars, the INDI-NMPC method achieves substantially smaller fluctuation ranges in both positional and attitude control compared to conventional PID methods. Through its adaptive INDI strategy, this approach maintains stable attitude dynamics

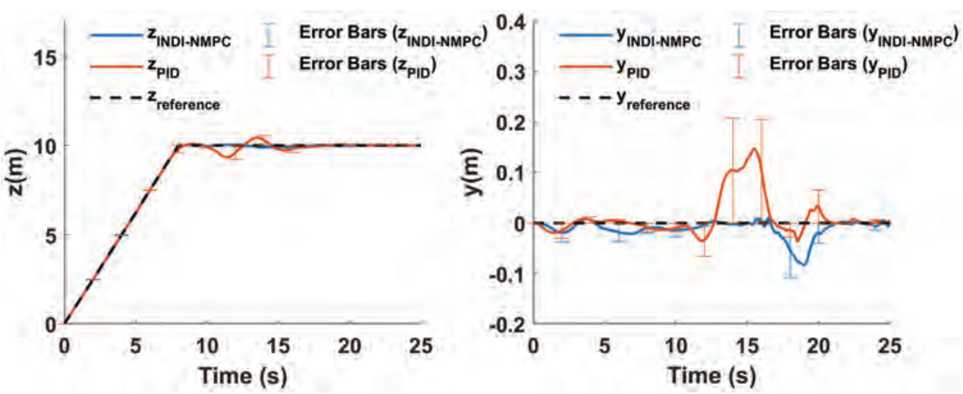

Fig. 9. Position comparison.

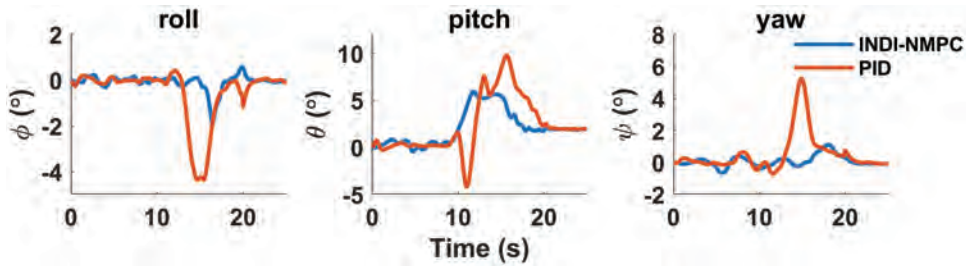

Fig. 10. Attitude comparison.

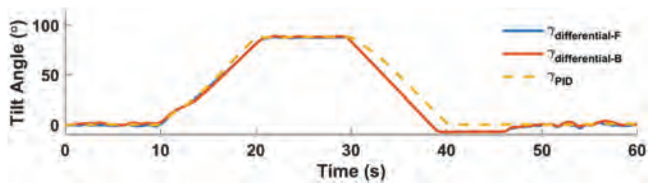

Fig. 11. Tilt angle comparison.

during rotor-tilt transitions, reducing the maximum attitude deviation by 42.59% relative to PID controllers. Furthermore, the proposed method enables rapid correction of lateral deviations while ensuring constant altitude throughout the tilt phase by employing a high weight cost function in its optimization framework.

4.2. *Dual differential model obstacle avoidance experiment*

After executing the tilt action and entering the fixed-wing mode, the TRUAV can optimize its maneuverability by switching from front-back differential mode to left-right differential mode. To demonstrate this, the following flight scenario is set: two obstacles are placed at heights of 10 m at positions of 200 m and 350 m, respectively. The aircraft must navigate around these obstacles by adjusting its flight path, circumventing them from above on the left and below on the right, respectively. During the obstacle avoidance process, differential tilting of the left and right propellers generates roll and yaw torques, thus successfully completing

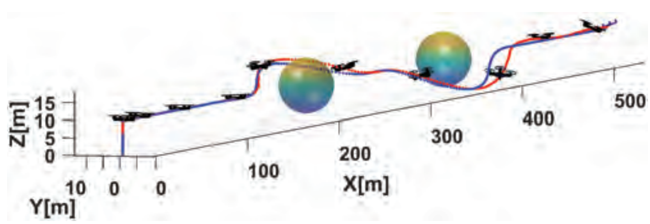

Fig. 12. Obstacle avoidance experiment (the red line represents the obstacle-avoidance flight trajectory under the influence of crosswind noise ($\mu = 0, \sigma = 0.5$), and the blue line represents the obstacle-avoidance flight trajectory without any disturbances).

the avoidance maneuvers. This differential control strategy effectively supports the TRUAV's agile flying and precise obstacle avoidance in complex environments. In the flight obstacle avoidance procedure of TRUAV, Gaussian white noise ($\mu = 0$ and $\sigma = 0.5$) was incorporated as a crosswind perturbation. This was done to elucidate the practical deployment performance of the adopted INDI-NMPC control method.

Flight test results show that when the TRUAV encounters obstacles and performs maneuvering for obstacle avoidance, the tilting angles of the left and right rotors are altered through differential changes to assist in the avoidance maneuvers. For instance, between 23 s and

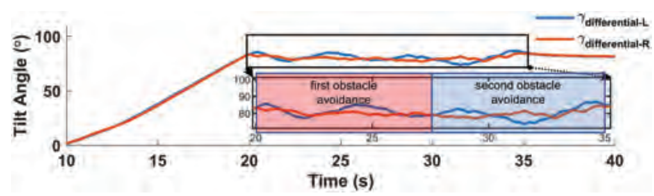

Fig. 13. Differential tilt angle.

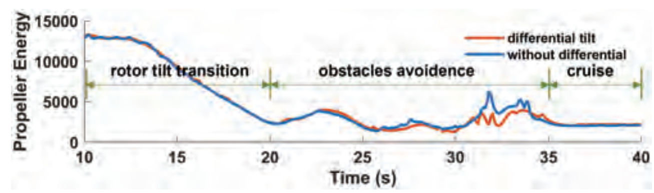

Fig. 14. Total propeller energy.

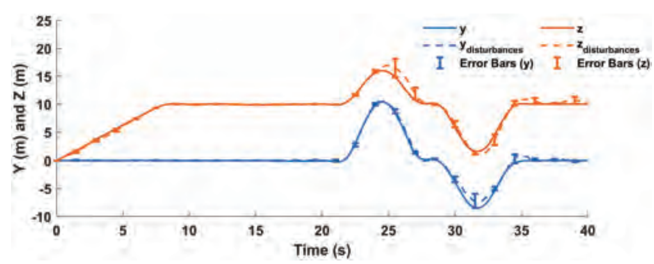

Fig. 15. Position of TRUAV during obstacle avoidance ($\mu = 0, \sigma = 0.5$).

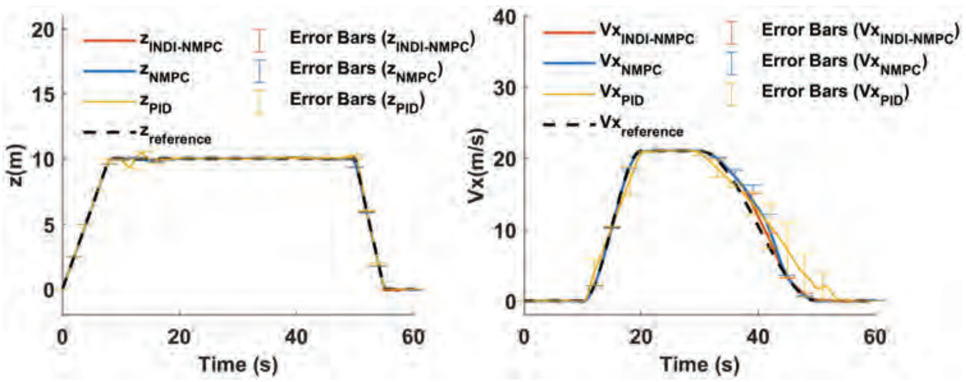

Fig. 16. Comparison of altitude and forward speed.

30 s, when the tilt angle of the left rotor is less than that of the right, the thrust direction of the left rotor is closer to the z-axis, thereby generating a positive roll torque on the x-axis, which aids the TRUAV in performing avoidance maneuvers toward the negative direction of the y-axis; conversely, when the tilt angle of the left rotor is greater than that of the right, the thrust direction of the left rotor is closer to the x-axis and the right rotor's thrust direction is closer to the z-axis, thereby producing a negative roll torque on the x-axis, as observed between 21 s and 22 s and 30 s and 33 s, as shown in Fig. 13. As shown in Figs. 12 and 15, the position trajectory exhibited measurable deviations from the perturbation-free baseline following the introduction of aerodynamic disturbances, yet maintained robust convergence to the nominal flight path, thereby validating the inherent robustness of the proposed control law.

Figure 14 shows that between 10 s and 20 s, as the TRUAV transitions from tilt mode to fixed-wing mode, both rotor speed and total energy significantly decrease. In rotor mode, the rotors not only counteract gravity but also provide the TRUAV with the acceleration needed for vertical takeoff. In fixed-wing mode, the wing's aerodynamic force is sufficient to counteract gravity, with the rotors only needing to provide a smaller forward pull force. This energy management across different flight modes significantly improves energy efficiency. Detailed force analysis graphs during this change are presented in Sec. 4.3, Fig. 19 of the flight tests. Therefore, the TRUAV demonstrates a higher potential for energy optimization compared to quadrotors, which is also believed by the team to be a key reason for its significant developmental progress.

Moreover, compared to the nondifferential mode, the TRUAV in differential mode can reduce rotor speed more effectively through more coordinated turning actions during maneuvering operations, thereby optimizing energy usage. Through quantitative analysis, the TRUAV with a dual differential architecture reduces energy consumption by 7.12% during the obstacle avoidance phase.

4.3. ***Full flight process experiment***

In the flight experiments, the TRUAV initially remained stationary on the ground, then took off vertically and hovered stably at an altitude of 10 m. After 10 s, the rotors began to tilt forward, and over the next 10 s, the forward speed was accelerated to 21 m/s while maintaining a fixed hovering altitude. Subsequently, the rotors tilted back, the aircraft began to decelerate, and eventually, the speed was reduced to zero as it hovered in the air. After completing the hover, the TRUAV descended vertically back to the ground.

The data shown indicate that the NMPC method can effectively complete the full trajectory tracking and attitude control of the tilt-rotor UAV. Compared to traditional PID, NMPC demonstrates superior capabilities in maintaining aircraft posture and prepares for future control actions through rolling prediction techniques. For example, when the TRUAV needs to accelerate, PID incorrectly treats the aircraft as a quadrotor model and adopts a head-down acceleration strategy, which often leads to overshooting in posture and fluctuations in altitude tracking, as shown in Figs. 16 and 17.

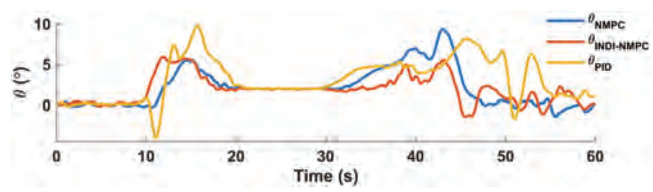

Fig. 17. Pitch comparison.

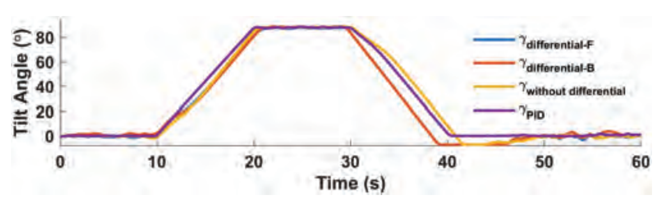

Fig. 18. Tilt angle comparison.

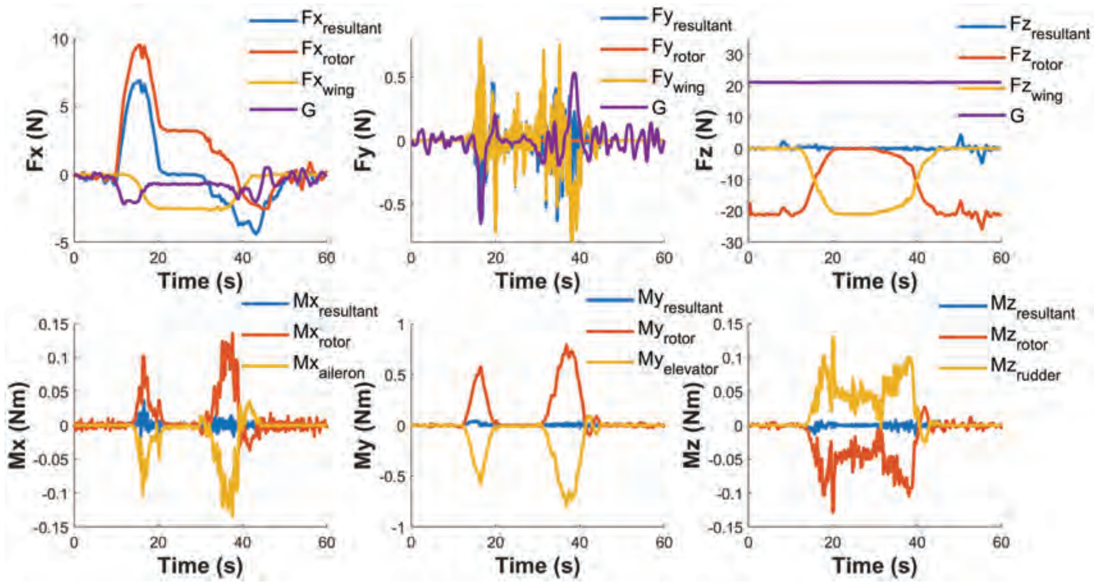

Fig. 19. Force and torque during the flight process.

In contrast, NMPC shows distinct advantages during deceleration, achieving faster deceleration and more stable posture maintenance.

Furthermore, unlike the fixed reference curves for tilt angles in PID and NMPC, INDI-MPC follows an adaptive tilt strategy guided by INDI, adjusting the tilt angle in real-time based on current speed and posture. By using a front-rear differential model, INDI-MPC reduces pitching actions during deceleration. According to Fig. 19, this study demonstrates the reasons for changes in position and attitude throughout the flight by analyzing the forces acting on the TRUAV. During flight, when rapid deceleration is necessary, the pitch adjustments of the TRUAV are minimal and are primarily regulated through aerodynamic forces on the wings and the gravitational component along the Z-axis. As the speed gradually decreases, the rotors tilt backward within the permitted constraints ($-7°$ to $90°$), compensating for the decrease in lift from the wings and generating a reverse force component to help the TRUAV quickly correct its position and maintain a hover, as shown in Fig. 18. Using the pitch angle variation throughout the entire flight process as a quantitative analysis metric, the proposed INDI-NMPC controller reduces the maximum pitch angle by 34.60% compared to PID and by 11.44% compared to the conventional NMPC method.

Flight experiment results show that the NMPC controller exhibits outstanding performance throughout the entire flight process compared to PID. The NMPC method effectively addresses control distribution issues, optimizes the coordination of propellers, wings, and control surfaces, ensuring TRUAV's trajectory tracking and attitude stability, while the adaptive tilt strategy of INDI further enhances attitude control effectiveness.

5. Conclusion

In response to the challenges posed by the dual differential rotor architecture and highly nonlinear mathematical model of the TRUAV for attitude control and tilt strategy design, an NMPC controller based on the INDI tilt strategy is proposed in this paper. Verified through flight experiments, the proposed controller effectively manages the complex full flight process of the TRUAV, including takeoff, tilt, level flight, reverse tilt, and landing, and excellently handles the continuously changing nonlinearity of the TRUAV. It adequately achieves control distribution, fully harnessing the aircraft's potential. Analysis of experimental results shows that the performance of the proposed controller is significantly superior to traditional PID and NMPC alone. In the dual differential model obstacle avoidance experiment, the model demonstrated its enhanced flight control capabilities, effectively optimizing energy usage and facilitating coordinated maneuvers.

ORCID

Tianrui Fang
https://orcid.org/0009-0001-2264-6182
Changping Du
https://orcid.org/0000-0003-0552-2492

Rui Yang
https://orcid.org/0009-0007-4012-690X
Yuean Wu
https://orcid.org/0009-0007-3503-420X
Jiahao Yu
https://orcid.org/0009-0007-5560-9648
Zean Du
https://orcid.org/0009-0001-7327-5692
Yiming Shang
https://orcid.org/0009-0004-1290-4610
Yao Zheng
https://orcid.org/0000-0003-2126-2897

References

[1] K. P. Valavanis and G. J. Vachtsevanos, *Handbook of Unmanned Aerial Vehicles* (Springer Publishing Company, 2014).
[2] O. Aedo, K. A. Barbosa and A. Álvarez, Mixed controller design for an UAV flight control system, in *CHILEAN Conf. Electrical, Electronics Engineering, Information and Communication Technologies* (*CHILECON*) (IEEE, 2015), pp. 135–140.
[3] L. F. Fernandez, M. Bronz, N. Bartoli and T. Lefebvre, Development of a mission-tailored tail-sitter MAV, *Unmanned Syst.* **12**(03) (2024) 611–625.
[4] G. Cai, J. Dias and L. Seneviratne, A survey of small-scale unmanned aerial vehicles: Recent advances and future development trends, *Unmanned Syst.* **02**(02) (2014) 175–199.
[5] J. Escareño, S. Salazar and R. Lozano, Modelling and control of a convertible VTOL aircraft, in *Proc. 45th IEEE Conference on Decision and Control* (IEEE, 2006), pp. 69–74.
[6] J. S. Boling, G. Zha and C. Zeune, A high-speed, high-efficiency VTOL concept using CoFlow Jet airfoil, in *AIAA Aviation 2020 Forum*, Virtual event (AIAA, 2020), p. 2792, https://doi.org/10.2514/6.2020-2792.
[7] C. Papachristos, K. Alexis and A. Tzes, Towards a high-end unmanned tri-TiltRotor: Design, modeling and hover control, in *20th Mediterranean Conf. Control and Automation, MED 2012 — Conf. Proc.* (IEEE, 2012), pp. 1579–1584.
[8] G. Flores, I. Lugo and R. Lozano, 6-DOF hovering controller design of the Quad Tiltrotor aircraft: Simulations and experiments, in *53rd IEEE Conf. Decision and Control* (IEEE, 2014), pp. 6123–6128.
[9] K. Muraoka, N. Okada, D. Kubo and M. Sato, Transition flight of quad tilt wing VTOL UAV, in *Proceedings of the 28th Congress of the Int. Council of the Aeronautical Sciences* (ICAS, Bonn, Germany, 2012).
[10] S. Schröter, E. Smeur and B. Remes, Design and joint control of a conjoined biplane and quadrotor, *Unmanned Syst.* **12**(03) (2024) 579–588.
[11] P. Hartmann, C. Meyer and D. Moormann, Unified velocity control and flight state transition of unmanned tilt-wing aircraft, *J. Guid. Control Dyn.* **40**(6) (2017) 1348–1359.
[12] C. Kikumoto, T. Urakubo, K. Sabe and Y. Hazama, Back-transition control with large deceleration for a dual propulsion VTOL UAV based on its maneuverability, *IEEE Robot. Autom. Lett.* **7**(4) (2022) 11697–11704.
[13] M. Sato and K. Muraoka, Flight controller design and demonstration of quad-tilt-wing unmanned aerial vehicle, *J. Guid. Control Dyn.* **38**(6) (2015) 1071–1082.
[14] E. Small, E. Fresk, G. Andrikopoulos and G. Nikolakopoulos, Modelling and control of a tilt-wing unmanned aerial vehicle, in *24th Mediterranean Conference on Control and Automation* (*MED*) (IEEE, 2016), pp. 1254–1259.
[15] L. Bauersfeld and G. Ducard, Fused-PID control for tilt-rotor VTOL aircraft, in *28th Mediterranean Conf. Control and Automation* (*MED*) (IEEE, 2020), pp. 703–708.
[16] A. Hamissi, K. Busawon, L. Dala, Y. Bouzid, M. Zaouche and M. Hamerlain, A new nonlinear control design strategy for fixed wing aircrafts piloting, *Unmanned Syst.* **09**(04) (2021) 293–308.
[17] W. Zhao and C. Underwood, Robust transition control of a Martian coaxial tiltrotor aerobot, *Acta Astronaut.* **99** (2014) 111–129.
[18] B. Xian, G. Jianchuan, Z. Yao and Z. Bo, Sliding mode tracking control for miniature unmanned helicopters, *Chin. J. Aeronaut.* **28**(1) (2015) 277–284.
[19] C. Ma, D. Sun and N. Hovakimyan, Modeling and adaptive control law design for a bi-tiltrotor unmanned aerial vehicle, *J. Aerosp. Eng.* **34**(6) (2021) 04021090.
[20] Y. Li, X. Liu, Q. He, R. Ming, W. Huang and W. Zhang, L1 adaptive structure-based nonlinear dynamic inversion control for aircraft with center of gravity variations, *J. Intell. Robot. Syst.* **106**(1) (2022) 4.
[21] S. K. Settar, N. A. Ahmed, F. F. Hatem and R. B. D. Mohd, Three phase induction motor torque ripple minimization based on a novel nonlinear dynamic inverse controller, in *Proc. National Conf. Postgraduate Research*, Vol. 321 (Universiti Malaysia Pahang, 2016), pp. 321–329.
[22] B. N. Pamadi, *Performance, Stability, Dynamics, and Control of Airplanes* (AIAA, 2004).
[23] X. Fang, Q. Lin, Y. Wang and L. Zheng, Control strategy design for the transitional mode of tiltrotor UAV, *IEEE 10th Int. Conf. Industrial Informatics* (IEEE, 2012), pp. 248–253.
[24] Z. Lin, Q. Liu, S. Liu and B. Yan, Transition controller design of tilt-rotor UAV based on incremental nonlinear dynamic inversion, in *IECON 2023-49th Annual Conf. IEEE Industrial Electronics Society* (IEEE, 2023), pp. 1–6.
[25] F. Allgower *et al.*, Nonlinear model predictive control: From theory to application, *J. Chin. Inst. Chem. Eng.* **35**(3) (2004) 299–316.
[26] A. Kovacs and I. Vajk, Optimization-based model predictive tube control for autonomous ground vehicles with minimal tuning parameters, *Unmanned Syst.* **11**(01) (2023) 93–108.